Investigating the performance of a novel solar lighting/heating system using spectrum-sensitive nanofluids[1]

Chao Shen[1,2]*, Guoquan Lv[1]*, Shen Wei[3], Chunxiao Zhang[1], Changyun Ruan[1]

1) School of Architecture, Harbin Institute of Technology, Key Laboratory of Cold Region Urban and Rural Human Settlement Environment Science and Technology, Ministry of Industry and Information Technology, Harbin 150090, China

2) State Key Lab of Subtropical Building Science, South China University of Technology, Guangzhou 510640, China

3) The Bartlett School of Construction and Project Management, University College London (UCL), London, WC1E 7HB, UK

Abstract: Solar lighting is considered as a promising technique, which has huge potential in conserving energy and relaxing the residents. However, current solar lighting systems used a filter to allow only visible light to enter buildings, releasing all the other energy contained in the long wave of the solar into the surrounding air. Such practice leaded to low efficiency of solar energy utilization and high costs. In this paper, a solar lighting/heating system was developed which used a hollow lens filled with ATO nanofluid to separate the long wave and short wave of solar energy. A series of tests were conducted to explore the performance of system. Results indicated that under the test condition of Case 1 (0.025%/0.0001% ATO/Graphite nanofluid, 100 L/h flow rate), the light transmission efficiency was 19.5% which was comparable to that of current solar lighting systems, and the heat absorption efficiency was 25.35%. The heat energy collected by the such a system from June to August (three months) in the city of Harbin was about 466.4 MJ in per square meter of collection area. The volume concentration of nanofluids had great influence on both the light transmission efficiency and the heat absorption efficiency. The flow rate had little influence on the light transmission efficiency, but had great influence on the heat absorption efficiency of the system.

Keywords: Solar energy, Daylighting, Thermal energy, Nanofluids.

* Corresponding author: Chao Shen, chaoshen@hit.edu.cn

* Corresponding author: Guoquan Lv, lgq_academic@163.com

The short version of the paper was presented at CUE2019, Oct 16-18, Xiamen, China. This paper is a substantial extension of the short version of the conference paper

Nomenclature

Abbreviations

A	Cross-sectional Area, m^2
c	Specific Heat Capacity, kJ/(kg·K)
E	Illumination, lux
G	Radiation Intensity, W/m^2
n	Refractive Index
Q	Quantity of Heat, W
t	Temperature, ℃
V	Flow Rate, m^3/s
ρ	Density, kg/m^3
θ	Angle
η	System Efficiency, %
ϕ	Luminous Flux, lm

Symbols

in	Inlet
out	Outlet
R	Solar Radiation

1 Introduction

Energy and environment are key for sustainable development of human cities and society [1], and have captured great attentions globally in recent years. Buildings have been widely acknowledged as a major energy contributor, leading to serious environmental issues. In China, buildings are responsible for 20%-25% of overall social energy consumption and more than 1/3 total CO_2 emissions [2]. In the USA, this number is even close to 40% [3]. Among all energy systems in buildings, artificial lighting takes a high percentage of overall building energy consumption. For example, in China, 12%-16% of national power is consumed by artificial lighting (629.4 billion kWh vs. 5245.1 billion kWh) [2].

In buildings, various lighting bulbs have been used, with different energy efficacy, color temperature etc. The luminous efficiency for incandescent lamps is only about 10 lm/W-15 lm/W, with a color temperature between 2400K to 2950K [4]. Fluorescent lamps give higher luminous efficiency than incandescent lamps, between 20 lm/W to 60 lm/W, with color temperature between 3000K to 6500K. Apparently, both incandescent lamps and fluorescent lamps are not energy efficient, in terms of the light intensity given by each power unit consumed (Watt). In recent years, LEDs (Light-Emitting Diodes) have been commonly used in buildings, due to their high energy efficacy (100 lm/W-200 lm/W) and wide range of color temperature [5].

Daylight can improve occupants' visual comfort and is good for occupants' health [6]. Using daylight more efficiently can also reduce the reliability of artificial lighting, hence saving building energy consumption [7]. Solar lighting systems have been developed for several years to transmit daylight into buildings using either light tubes or optical fibers, with the latter one being more popular due to its ability of long-distance light transmission [8]. These systems use solar collectors, like Fresnel lens, to capture high-intensity daylight and transmit it into indoor environment through optical fibers. Although this system is sustainable and energy efficient (the ideal computational efficiency is about 35%-40% when the transmission distance was 10m [9]), a major issue it has is the extreme high heat accumulation at the connection between the lens and the optical fibers, and this heat will raise the temperature of optical fibers. When the temperature is higher than the melting point, it will damage the optical fiber.

To solve this issue, many researchers have provided their solutions [8-14]. One major solution to this issue is using appropriate filters to redirect infrared radiation energy back to the ambient environment [10-14]. The first optical fiber solar lighting system in the world, namely, Himawari, just uses this method to protect optical fibers from melting by accumulated heat [10]. Using this method, however, the transmittance of filter to visible light was only between 80% to 90% [15], and there were fiber coupling loss, bending loss and other loss occurred in actual operation, so the overall light transmission efficiency would be reduced to between 19% and 25% (the transmission distance was 10m) [13,16]. Based on this solution, some studies have added additional designs, such as varying the size of the concentrators and optical fibers [8,13] and using silicon fibers (with a higher melting temperature) at the beginning and plastic fibers for optical transmission [10], to promote the performance.

Existing solutions, however, all try to limit the negative effects of infrared radiation, but not to reuse it. This leads to great waste of energy as infrared radiation accounts for 47% energy of sunlight [17]. In this study, a novel solar lighting/heating system has been developed to promote the energy efficiency of existing solar lighting systems by reusing the energy from infrared radiation to heat domestic hot water. The system can realize the function of cascading utilization of solar radiation in different bands and spectrum-sensitive nanofluids have been used to filter solar energy with different bands [18]. This paper has described the development of this novel lighting/heating system in Chapter 2. Chapter 3 introduced experimental apparatus that have been used to test the performance of the new system, as well as testing procedures. Chapter 4 mentions major testing results in terms of the system performance and plus a preliminary energy-saving assessment about its ability of recovering infrared radiation energy. Some major findings from this study have been summarized the conclusion section of this paper.

2 System Development

Fig. 1 has depicted a basic schematic of the solar lighting/heating system proposed in this study, with two major outputs, namely, one for indoor lighting and another for heating domestic hot water. In this system, the major collection of solar energy is achieved by the solar energy collector, as shown in Fig. 1. It has a Fresnel lens to concentrate solar radiation and behind this is a hollow lens. When passing through the hollow lens, visible light will be transmitted to indoors through optical fibers and infrared solar energy will be absorbed by the pass-by nanofluid and then used to heat domestic hot water through a heat exchanger. In order to obtain a higher energy efficiency of the system, the solar lighting technology with concentrator was used to concentrate the sunlight before it enters the light components of optical fiber bundle [8].

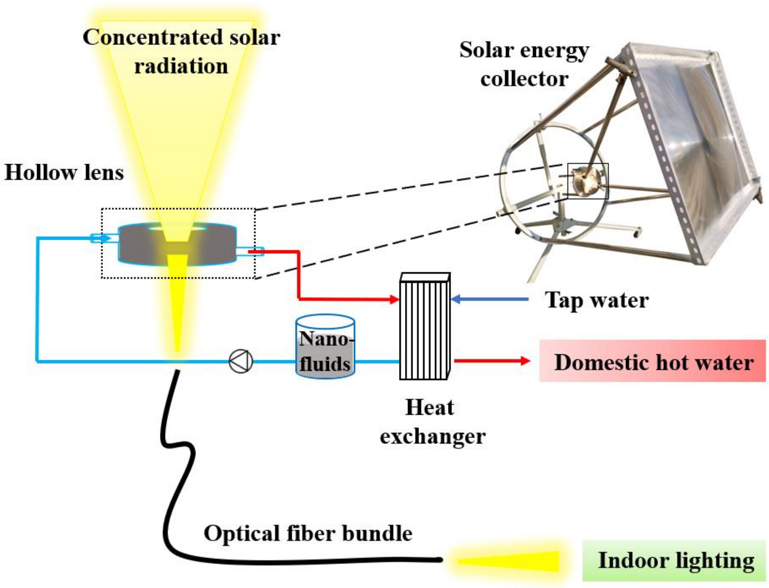

Fig. 1. Schematic diagram of solar lighting/heating system.

2.1 Design of hollow liquid-filled lens

In this study, a Fresnel lens has been used to concentrate solar radiation, and this lens is a common type and no special treatment is needed. The hollow lens, however, needs special design to enable transmission of visible light (for lighting provision) and pass-through of nanofluid (for heat provision). In this lens, there is a large cavity, with one fluid inlet and one fluid outlet on both sides. This is the path for nanofluid to absorb infrared solar energy. Fig. 2 has shown dimensions and real picture for the hollow lens designed in this study. Inside the cavity, there is a cone-shaped hollow, with bigger opening on the top and smaller opening at the bottom at a cone base angle of 45°. The hollow lens was made of quartz glass with the refractive index (n=1.5) which is greater than that of air (n=1.0). According to the refraction law, the angle between the incident light and the vertical direction will be reduced when the light passes through the cone plate, which means the light will be concentrated and is favorable to an efficient light transmission in the optical fiber [19]. For the silicon fiber with smaller NAs (numerical aperture) of 0.2-0.37, the light transmission efficiency is higher than this Case. This design has been justified in many existing studies as having advantages in providing optimized incidence angle for entering the optical fiber [16,20].

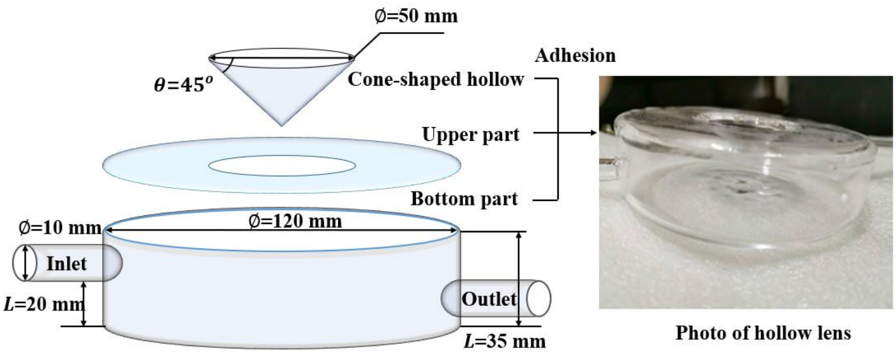

Fig. 2. Structure diagram of hollow lens and its photo.

2.2 Selection of nanofluids

Nanofluid is a kind of stable suspension formed by dispersing small particles under 100 nm in a base solution. Due to their small size and large specific surface area of particles, nanofluids have much different physical and chemical properties than base solution fluids [21]. By changing materials of nanoparticles and their size, concentration and shape [22], nanofluids can absorb the part of sunlight with specific frequency band [23,24].

In the system proposed here, nanofluid is acting as a medium between solar radiation and domestic hot water. It is expected that in comparison with the existing solar lighting systems without thermal energy utilization, the proposed system could recover the heat energy of infrared sunlight to heat domestic hot water, and meanwhile, has the same light transmission efficiency (19%-25%, optical fiber transmission distance of 10 m). Therefore, the system needs nanofluids with high transmission for the visible light and high absorption for the infrared band. ATO (Antimony Tin Oxide) nanofluid is very suitable for these requirements. Many researchers have studied its characteristics [25,26] which could provide reference for this study. There are many literatures about the preparation method and spectral characteristics of ATO nanofluid. The price of ATO nanofluid is also very viable.

So, in this study, the ATO with two volume concentration has been selected and a small amount of graphite particles (0.0001% volume) have been mixed to enhance its absorption ability for solar radiation between 800 nm to 1000 nm. As shown in Fig. 3, nanofluid with the volume concentration of 0.025% ATO plus 0.0001% graphite has the same transmittance as single filter in the visible light band, and has the higher transmittance than double filter. Although the transmittance of 0.025%ATO plus 0.0001% Graphite in visible light band was lower than that of double filter, the absorption capacity of nanofluid in infrared band was enhanced. The data of filters in the figure is from the research results of Kandilli [15]. The transmittance of nanofluids was measured by uv-vis infrared spectrophotometer.

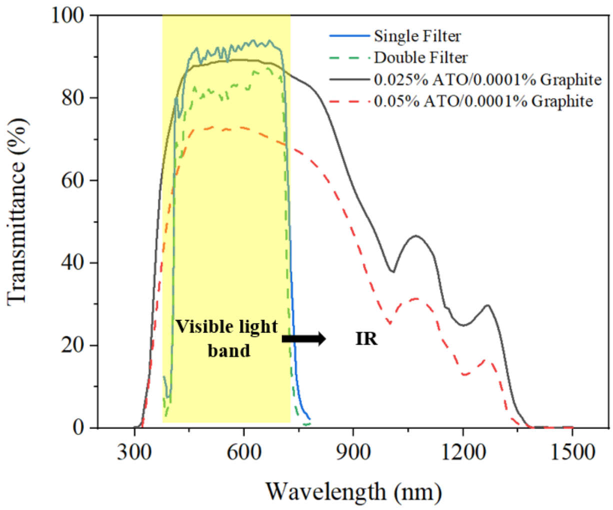

Fig. 3. Transmittance curves of nanofluids and fliters.

3 Methodology

3.1 Experimental design

To test the performance of this novel solar lighting/heating system, an experiment has been set up, as shown in Fig. 4. This testing kit collects some solar radiation outdoors and this solar radiation will pass through the Fresnel lens, and then the hollow lens. The

Fresnel lens had a cross-sectional area of 500 mm×500 mm, a focal length of 600 mm, a concentration ratio of 1000. The specific parameters of the hollow lens is described in Section 2.1. The distance from the cone top of hollow lens to Fresnel lens is equal to the focal length of the Fresnel lens, to ensure the concentrate solar radiation with maximum energy density (minimum cross-sectional area) enters into the hollow lens. Visible light will be transmitted through plastic optical fibers with the length of 10 m, and the transmission loss of 200 dB/km, to indoors and infrared solar energy will be absorbed by ATO/graphite nanofluid. To justify the performance of this system, some important parameters have been monitored and collected. Before the Fresnel lens, one solar power meter was used to measure the total amount of solar energy going into the testing kit. Additionally, an illumination photometer was used to measure the total amount of solar direct illumination. Three temperature sensors have been used in this test, one located at the inlet of optical fiber bundle to monitor the inlet temperature (making sure the temperature won't go beyond the fiber's melting temperature), one located on the flow path of the nanofluid system and another one located on the return path. These two readings were used to calculate the amount of heat absorbed by nanofluid. Lastly, there was an integrating sphere located inside the optical fiber bundle to decide how much daylight the system has transmitted. Table 1 has listed some important specifications for the measurement system, and Table 2 presents the information of the main components of this test system.

Table 1

Testing apparatus, accuracy and measurement intervals

Parameter	Test equipment	Accuracy	Measurement intervals
Temperature	Pt100	±0.05℃	30 seconds
Flow rate	Flowmeter	±0.1%	5 minutes
Illumination	Illumination photometer	±3.0%	5 minutes
Illumination flux	Integrating sphere	±3.0%	5 minutes
Radiation	Solar power meter	±5 W/m^2	5 minutes

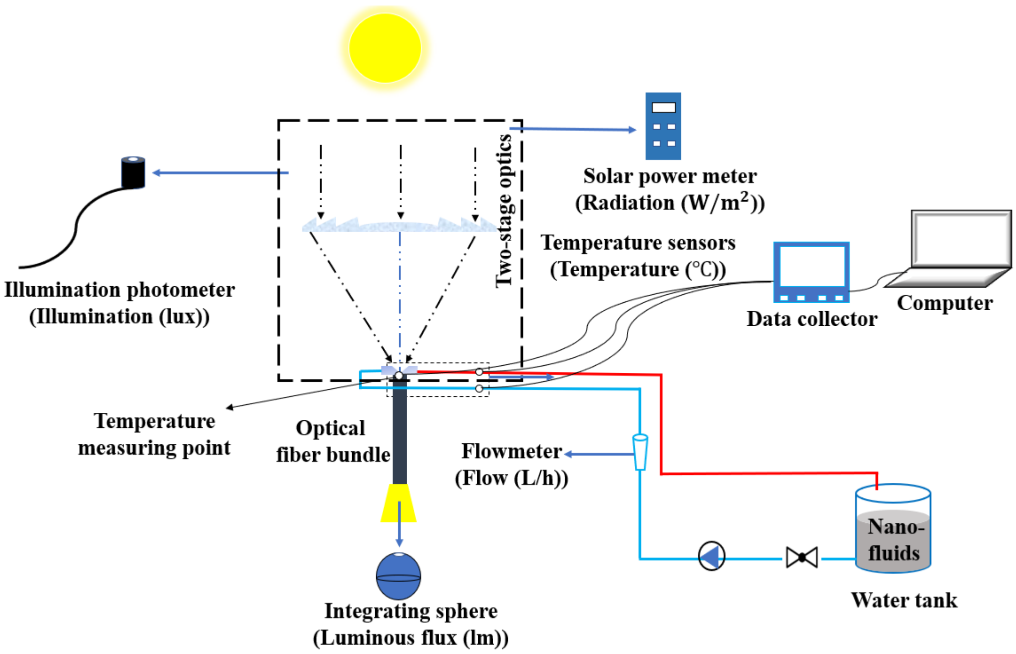

Fig. 4. Schematic diagram of experimental data acquisition location.

Table 2
Properties of system components

Component	Property	Value
Fresnel lens	Cross-sectional area	500 mm×500 mm
	Focal length	600 mm
	Concentration ratio	1000
	Material	PMMA(n=1.49)
Hollow lens	Dimension	Described in Section 2.1
	Material	Quartz glass(n=1.50)
Optical fiber	Cross-sectional area	Single diameter 2 mm
		Bundle diameter 30 mm
	Length	10 m
	NA(numerical aperture)	0.5
	Transmission loss	200 dB/km

3.2 Data collection

To test the performance of the proposed system, the experiment introduced above (Section 3.1) was carried out between 13:30-16:00 on 15 August, 2019, in Harbin, China (127° east longitude, 45° north latitude). The data was collected in the season with the highest solar radiation intensity in a year. Based on historic data collected by nearby weather stations, one of the highest periods of both direct solar illumination and solar radiation would be between 13:30 and 14:00 [27]. During this study, both these two parameters were monitored and recorded at an interval of five minutes during the testing period, and Fig. 5 has depicted both values based on an average of every half an hour. During the monitoring period, the average direct solar illumination was between 42200 lux and 57400 lux, and the average radiation intensity was between 982 W/m^2 and 1299 W/m^2. Table 3 has listed some basic experimental conditions.

Table 3
Experimental conditions

Parameter	Value
Rate of flow	100 L/h
Volume concentration of nanofluid (%)	Size 50 nm Volume concentration (0.025% ATO plus 0.0001% Graphite nanofluids)

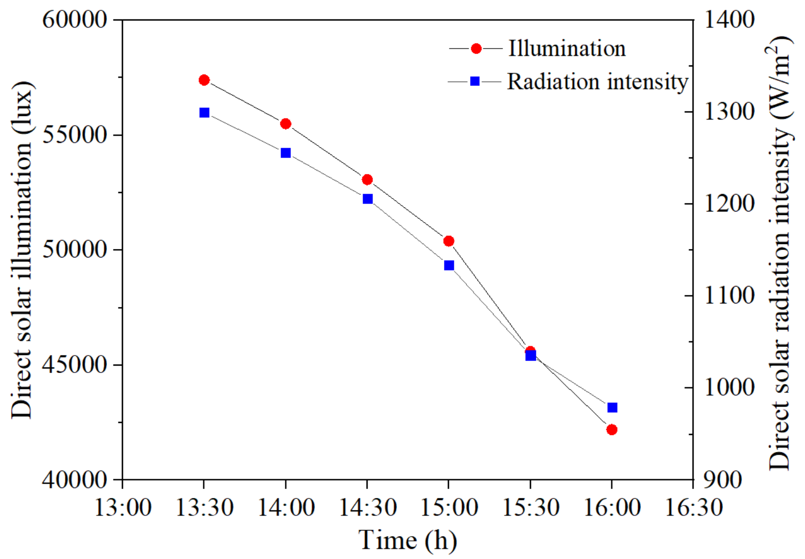

Fig. 5. Monitored direct solar illumination and intensity of direct solar radiation.

3.3 Performance indicator

Fig. 6 has depicted some important parameters that have been used in this study to confirm the performance (illumination efficiency η_i and heat absorption efficiency η_h) of the new system, including solar direct radiation intensity G_R, solar direct illumination E_R, luminous flux and energy input to the system ϕ_{in} and Q_{in} and output of these two parameters ϕ_{out} and Q_{out}.

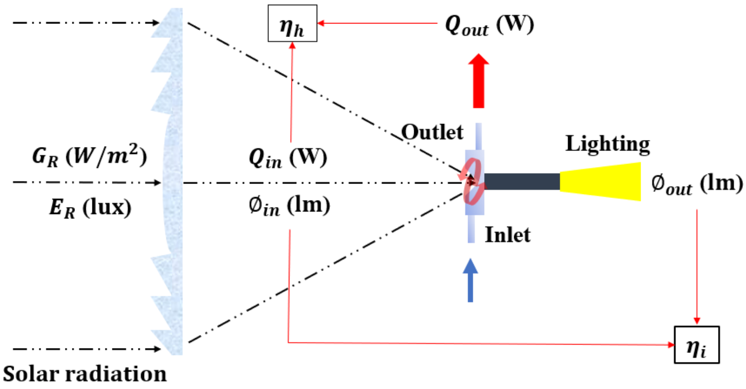

Fig. 6. Important parameters used to confirm the performance of the system.

In this testing, the total solar luminous flux going into the system is calculated by Eq. 1 [28],

$$\phi_{in} = E_R A_{\text{lens}} \tag{1}$$

where A_{lens} is the area of Fresnel lens (in m^2)

Therefore, the illumination efficiency, η_i, of the system could be defined by Eq. 2,

$$\eta_i = \frac{\phi_{out}}{\phi_{in}} \tag{2}$$

where ϕ_{out} is obtained by the integrating sphere.

Similarly, the total solar energy going into the system is calculated by Eq. 3 [12],

$$Q_{in} = G_R A_{lens} \tag{3}$$

The heat absorbed by the system, Q_{out}, could be calculated by the temperature difference and flow rate within the nanofluid loop, as defined in Eq. 4,

$$Q_{out} = c \cdot \rho \cdot V(t_{out} - t_{in}) \tag{4}$$

where c is specific heat capacity of nanofluids (in $\text{kJ/kg} \cdot \text{K}$), V is volume flow (in L/h), ρ is density of nanofluids (in Kg/m^3), t_{out} is nanofluid outlet temperature (in °C) and t_{in} is nanofluid inlet temperature (in °C).

Therefore, the heat absorption efficiency, η_h, of the solar lighting/heating system could be defined by Eq. 5,

$$\eta_h = \frac{Q_{out}}{Q_{in}} \tag{5}$$

4. Results and Analysis

4.1 Performance justification

As mentioned above, one of main purpose of this solution is to keep the inlet temperature of optical fiber bundles lower than their melting temperature, thus which were monitored during the experiment period and results are shown in Fig. 7. Apparently, the inlet temperature of fiber was kept far below its melting temperature, 140℃, to ensure its feasibility and reliability of such a system. Additionally, it also gives a possibility to the larger size of concentrators to collect more solar energy and reduce the economic cost for per unit of energy obtained by the system.

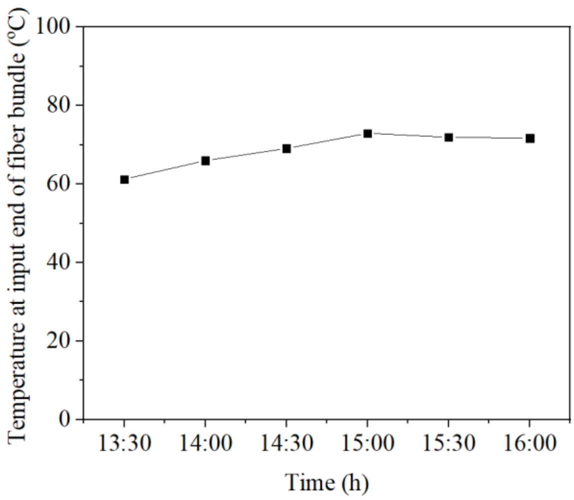

Fig. 7. Monitored inlet temperature of optical fiber bundle.

The solar luminous flux at the inlet of the Fresnel lens and the luminous flux at output end of the optical fiber bundle were tested, and thus, the light transmission efficiency η_i of the proposed solar lighting/heating system was calculated by Eq. 1 and 2. All the test results are shown in Fig. 8. As seen, the system's light transmission efficiency did not fluctuate greatly with the changing of outdoor illumination. The average light transmission efficiency was 19.5% which was similar to other solar lighting system without using nanofluids [13, 16].

In such a system proposed in this study, the nanofluids absorbs mainly the solar radiation that has thermal effect, but also absorbs a very little amount of visible light that was desired to pass through the hollow lens. However, it can be seen from Fig. 3, the transmissivity in visible light band of nanofluid used in this experiment is the same as that of filters used in conventional solar light system. In addition, the principle that optical fiber can transmit electromagnetic waves efficiently was the law of total reflection. The electromagnetic waves need to be less than the maximum incidence angle θ_{max} (determined by the NA of the optical fiber) into the optical fiber [15]. As shown in Fig. 9, the cone-shaped design of hollow lens can reduce the concentrated angle of the sunlight because of refraction law, and ensure all light into the optical fiber bundle less than the maximum incidence angle θ_{max}. Since the system performed stable light transmission efficiency, its output luminous flux became lower when approaching to the sunset time. However, even at 16:00, this system could also provide an output of 2100 lm luminous flux, which is sufficient for a 20 m^2 room. To serve a larger room, a bigger Fresnel lens and more fiber bundles are required to provide enough luminous flux.

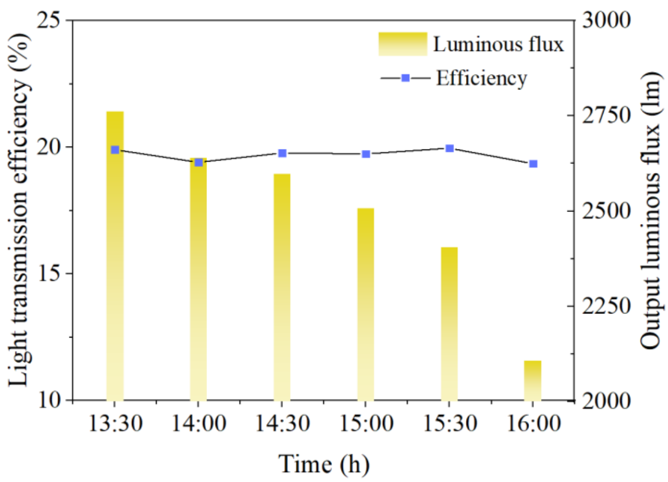

Fig. 8. System's light transmission efficiency and output luminous flux.

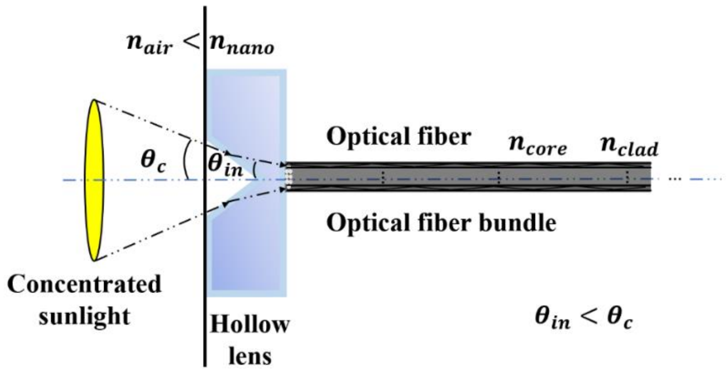

Fig. 9. Schematic diagram of system's optical path.

Fig. 10 shows the heat absorption efficiency of the experimental system that calculated by Eq. 3 to 5. As seen, the heat absorption efficiency of the proposed system decreased slightly with time changing from 13:30 to 16:00. This phenomenon was caused by many reasons. First, as the test time went on, the direct solar radiation intensity gradually decreased from 1299 W/m^2 at 13:30 to 982 W/m^2 at 16:00 (Fig. 5), and the heat energy absorbed by the nanofluid decreased gradually. Second, as seen from Fig. 11 that during this period, the temperature of nanofluid at the inlet of the hollow lens increased by ~20°C (from 28.7°C at 13:30 to 48.5°C at 16:00), while the outdoor air temperature decreased slightly, and the decrease was far less than 20°C. As a result, the temperature difference between the nanofluid and the outdoor air increased, causing an increasing heat loss. However, in the whole experimental period, the heat absorption efficiency of the system was only reduced from 26.8% to 24.4% (the average efficiency was 25.35%), indicating the system had a good performance in the heat preservation. In addition, compared to the corresponding parameters at 14:00, the heat absorption efficiency at 14:30 was slightly higher, the inlet temperature of nanofluid was higher as well, but the outdoor air temperature was lower, suggesting the heat loss of hollow lens was more sensitive to the outdoor air temperature than other natural environmental parameters. During the 2.5 hours test period, the system absorbed 786 kJ heat totally through the nanofluid in the hollow lens, which could raise the temperature of 20 L water by 10°C. Authors believed that a higher heat output could be achieved by increasing the area of the solar collector by such a proposed system.

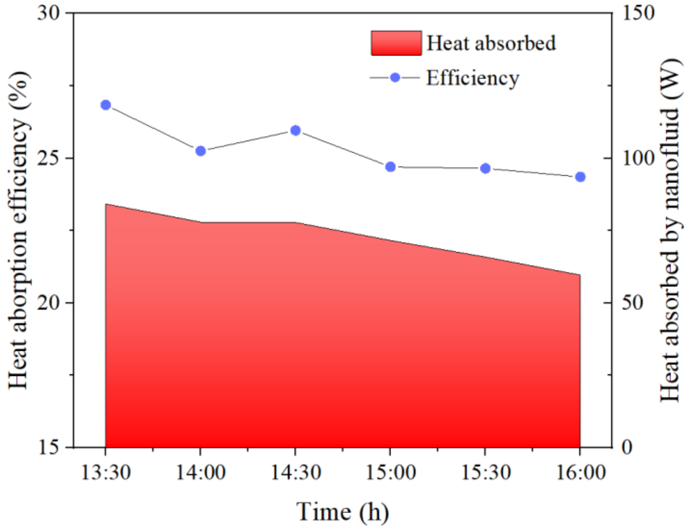

Fig. 10. Heat absorption efficiency and the amount of heat absorbed by nanofluid.

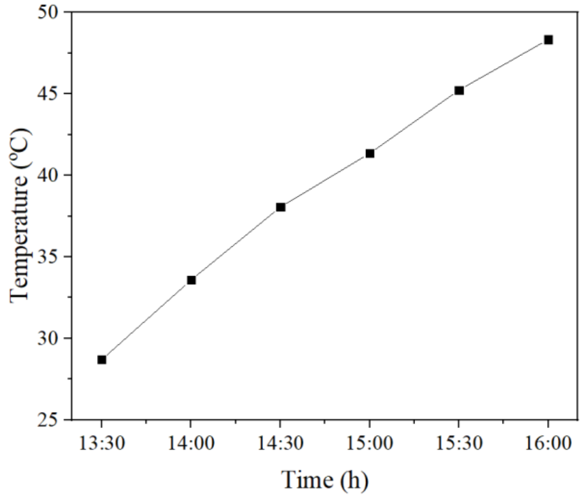

Fig. 11. Monitored inlet temperature of nanofluid.

Results in Section 4.1 indicated that the solar lighting/heating system proposed in this paper could realize that using solar energy in different bands separately to meet the different needs (light and heat), as a result, achieve a high energy efficiency. In addition, Chong [9] has studied a solar lighting system with optical fiber to transmit sunlight. The research results suggested that it was much more efficient to use sunlight directly than that to convert sunlight into electrical energy for lighting. The system proposed in this study provided a cascade utilization way of full-spectrum solar energy, to achieve co-production of solar lighting and domestic hot water. It used a low-cost way to recover infrared radiation energy, and thus enhance the market competitiveness of solar lighting technology.

4.2 Contribution to heating demand of domestic hot water systems

The solar radiation energy is mainly concentrated in the range of 300-3000 nm light wave, accounting for 99% of the total solar radiation energy. Of them, the visible band shares the percentage of 47%, the infrared band accounts for about 46%, and other accounts for 7%. The energy consumption of lighting accounts for about 16% of the total building energy consumption, and the energy consumption of domestic hot water accounts for about 14% [2]. As seen, the ratio of energy consumption for lighting to that for producing domestic hot water is 8:7 (16%:14%) and the ratio of visible light (for lighting) and infrared energy (for thermal energy) in solar radiation is 47:46 (47%:46%), thus the energy distribution for different function of the solar energy and the requirements of buildings are matched well generally. In addition, the experimental results reported by Lingfors [13] showed that the solar light system could provide light with higher luminous efficiency than the electric lighting. Therefore, such a system proposed in this study is suitable for application on buildings.

As verified in Section 4.1, this system has the transmission efficiency of visible light of 19.5% (Section 4.1) which is the similar as that of the conventional solar lighting systems, but can obtain the useful thermal energy additionally. In other words, the energy saved by this system was that used to produce domestic, in comparison with conventional solar lighting system. In this section, an assessment has been made to justify its contribution to energy saving in producing domestic hot water. Assuming that the system was used in Harbin, China (127° east longitude, 45° north latitude) and the average heat absorption efficiency of 25.35% (Fig. 9) was used. The energy-saving benefits was evaluated based on that 1 m^2 solar energy collection area of such a lighting/heating system.

In Harbin, the average annual sunshine hours is 2760 hours, and the average annual solar radiation amount is 4950 MJ/m^2 [29]. The total solar radiation from June to August (summer season, consistent with the time of experiment) was 1840 MJ/m^2. Taking the heat absorption efficiency of 25.35% of this lighting/heating system, the heat obtained in summer (June to August) by such a system with 1 m^2 collection area (Fresnel lens) installed in Harbin would be 466.4 MJ, which can heat 2220 L of tap water from 15℃ to 65℃. In other words, the system (1 m^2 collection area) could provide an average of 24.15 L of domestic hot water with the temperature of >65℃ per day in the test season. Although this is a preliminary calculation, it is enough to show the economic value and importance of this part of recovered thermal energy. What is more, using additional equipments to utilize the solar energy for lighting/heating of buildings could provide a good synchronous energy-saving benefit.

4.3 Effect of parameters on the system performance

In this section, four sets of experiments (based on the experimental set-up in Section 4.1) were carried out to explore the influence of flow rate and volume concentration of nanofluid on the output efficiency of this system. As shown in Table 4, Cases 1 and 3 had the same flow rate of 100 L/h, but different volume concentrations of nanofluids, 0.025% and 0.05%, respectively. Similarly, Cases 2 and 4 were conducted at the same flow rate of 50 L/h, but different volume concentrations of nanofluid, 0.025% and 0.05%, respectively. The test conditions are summarized in Table 4.

Table 4

Test condition with variable of flow and concentration.

Parameter		Case 1	Case 2	Case 3	Case 4
Flow rate (L/h)		100	50	100	50
Volume concentration of nanofluid (%)	ATO	0.025	0.025	0.05	0.05
	Graphite	0.0001	0.0001	0.0001	0.0001

Fig. 12 and 13 show four sets of monitoring data of direct solar radiation intensity and direct solar illuminance in Harbin, China (127° east longitude, 45°north latitude). Among them, the monitoring period of Case 1 and Case 2 was 13:30-16:00, and the monitoring period of Case 3 and Case 4 was 8:30-11:00. As seen, the values of the monitoring data of the four sets of experiments were similar basically. The values of the direct solar radiation intensity were all in the range of 900 W/m^2 - 1300 W/m^2, and the direct solar illumination was in the range of 40000 lux - 60000 lux. It shows that all these experiments were conducted under similar meteorological conditions.

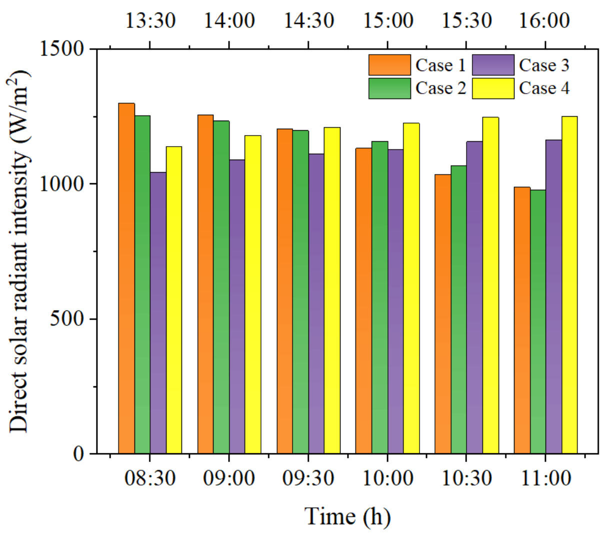

Fig. 12. Monitored direct solar radiation intensity in four sets of experiments.

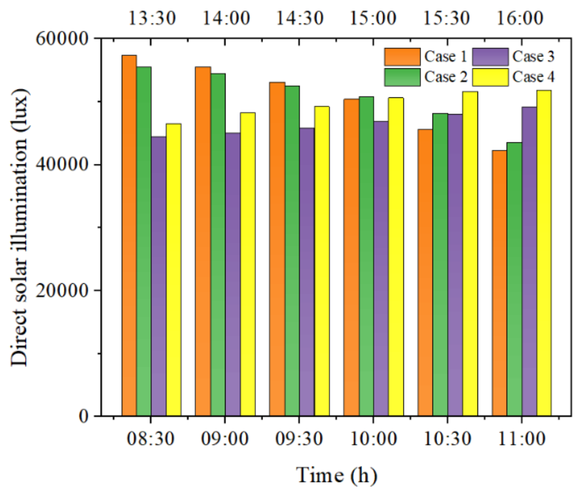

Fig. 13. Monitored direct sun illumination in four sets of experiments.

4.3.1 Effect of flow rate

Flow rate is an important factor affecting heat transfer and changing the arrangement order of nanoparticles in nanofluids, thus affecting the spectral transmittance [30]. Fig. 14 shows the experimental results of the light transmission efficiency in four Cases. Comparing Cases 1 and 2, Cases 3 and 4, it could be found that the flow rate had little effect on the light transmission efficiency. One reason for this phenomenon would be that the spatial posture of nanoparticles in the fluid was not affected by the increase of flow rate. Another reason was that the nanoparticles used in this study was spherical, one-dimensional shape, with the same scattering and absorption effect on electromagnetic waves from all directions, as shown in Fig. 15. Therefore, the light transmission efficiency was almost constant with the change of flow rate. In the other words, flow rate of nanofluid did not affect the light transmission efficiency.

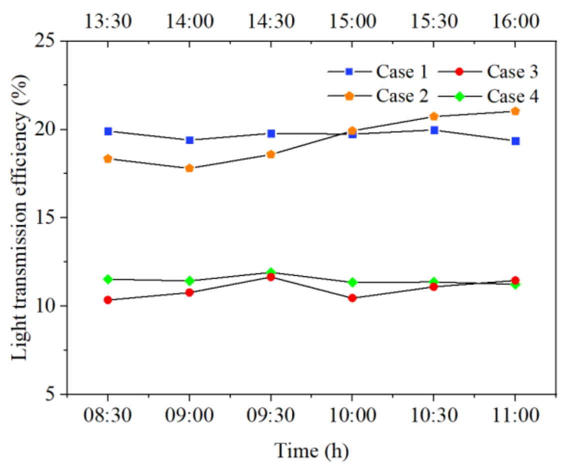

Fig. 14. Light transmission efficiency in four sets of experiments.

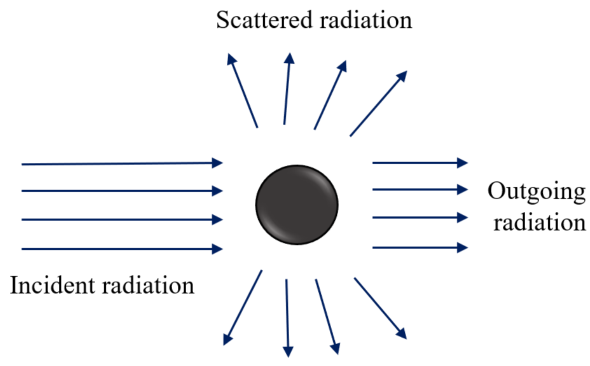

Fig. 15. Scattering diagram of spherical particles.

The experimental results of heat absorption efficiency are shown in Fig. 16. The comparisons between Cases 1 and 3, and between Cases 2 and 4 indicated that the flow rate had a significant effect on the heat absorption efficiency of this system. The increase of flow rate would increase the disturbance of nanofluid inside the lens, and thus, improve the heat transfer between the fluid and the lens wall. Therefore, the heat accumulated in the lens wall and that absorbed in the nanofluid could be effectively carried away by nanofluid, as a result, the heat absorption efficiency was enhanced and the heat loss from the hollow lens to the environment was reduced.

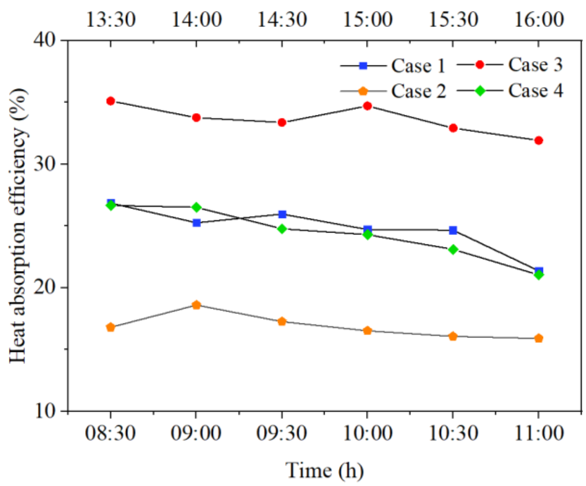

Fig. 16. Heat absorption efficiency in four sets of experiments.

In addition, comparing the visible light transmission efficiency and heat absorption efficiency in Cases 1 and 2, it can be found that the visible light transmission efficiency of these two Cases was almost the same, but the heat absorption efficiency in Case 1 was about 10% higher than that in Case 2. It indicated that a large amount of heat could store in the hollow lens wall, and when the flow rate was low, the nanofluid could not carry away the heat in time, which caused the heat being released into the environment in vain. One suggestion was recommended here, the inner wall of the hollow lens could be made into the fold shape like the Fresnel lens, which can increase the disturbance of the nanofluid inside the lens and promote the heat gain of the nanofluids.

4.3.2 Effect of volume concentration

The volume concentration of nanofluids determined the number of nanoparticles contained in the unit volume of fluid, which had a direct impact on the physical properties of nanofluids [31]. As shown in Fig. 14, the visible light transmission efficiency in Cases 1 and 2 (about 19.5%) was much higher than that in Cases 3 and 4 (about 11%). This is because the higher nanofluid volume concentration means more nanoparticles were contained in the nanofluid, thus the scattering and absorption on electromagnetic wave would be enhanced in nanofluid [32]. Consequently, the amount of sunlight passed through the hollow nanofluid lens decreased significantly when nanofluid volume concentration increased from 0.025% to 0.05%.

By comparing the heat absorption efficiency in Case 1 to Case 3, and Case 2 to Case 4, the increase of volume concentration in nanofluid had a significant improvement on the heat absorption efficiency, which could be explained from two aspects. First, the increase of nanofluid volume concentration could change the thermal physical properties of the fluids, thus increased the thermal conductivity, viscosity, heat transfer coefficient, specific heat capacity, etc [31]. Second, the amount of nanoparticles in the fluid was increased apparently, making more solar energy was absorbed by the nanofluid, thus the absorption ability of nanofluid on the solar radiation was greatly enhanced.

The experimental results suggested that both the flow rate and the volume concentration of nanofluid could affect the energy output efficiency of this system. Therefore, the system should be operated with the optimal operating mode according to the energy demand characteristics of the building and the local climate conditions in practical applications.

5 Future research

The solar lighting/heating system proposed in this paper can realize the comprehensive utilization of the whole solar spectrum. Experimental results showed that the proposed system had the same light transmission efficiency to that of existing solar lighting systems, but could provide additional heat energy, thus the total energy efficiency was higher than previous systems. As known, operating conditions have a great impact on the system efficiency, such as, the effect of volume concentration and flow rate of nanofluids was discussed in Section 4.3. In addition, the configuration of the system itself has also a significant impact on the its performance. If an ideal nanofluid with full visible transmission and full infrared absorption could be made, the light transmission efficiency would be increased by about 10%, and the heat absorption efficiency could be increased by 15%-20%. Many researchers are working on this research, because it is required by many other solar energy utilization technologies. Moreover, the energy loss of optical fiber during the light transmission is another important factor affecting the system efficiency. If silicon optical fiber (transmission loss 20 dB/km-30 dB/km) was used as the transmission component, the light transmission efficiency could be greatly improved. However, the price of silicon fiber is much more expensive than plastic fiber used in this study. The purchase price of plastic fiber bundle in this paper was $62.2, but the price of silicon fiber bundle with the same specification is more than $995.6. The total cost of the test system in this study (excluding the cost of the sun tracking device) was only $381.8. Therefore, silicon fiber was recommended to utilize as the light transmission component to improve system efficiency if the economy is available, such as, in a long-life service system. Generally speaking, this paper made an exploration about recovering the infrared heat energy which was not considered in the traditional solar lighting system. The proposed system could be optimized with further research.

6 Conclusions

In this paper, a novel solar lighting/heating system was proposed, which worked for lighting of buildings like conventional solar lighting systems, and also, provided additional heat for domestic hot water heating. A series of tests were carried out to investigate its performance and how the related factors influence the performance. In Case 1, the light transmission efficiency of the system was 19.5%, which was the same as that of the current solar lighting system, but it provided an additional 25.35% of the photothermal conversion efficiency due to the recovery of heat energy of the infrared sunlight. The energy evaluation suggested that the heat energy recovered by the proposed system could produce the considerable economic value. Specifically, the quarterly heat obtained by such a system with 1 m2 collection area installed in Harbin would be 466.4 MJ (summer season). The volume concentration of nanofluids had great influence on both the light transmission efficiency and the heat absorption efficiency. The flow rate had little influence on the light transmission efficiency, but had great influence on the heat absorption efficiency of the system. The proposed system achieved the gradient utilization of solar sunlight for both space lighting and water heating in one device, thus had a higher energy efficiency in comparison with previous solar lighting system.

Acknowledgment

The authors gratefully acknowledge the funding support from the State Key Laboratory of Subtropical Building Science (Project#: 2020ZB15).

Reference

[1] Zhang Q , Xu J , Wang Y. Comprehensive assessment of energy conservation and CO^2, emissions mitigation in China's iron and steel industry based on dynamic material flows. Applied Energy 2018;209:251-265.

[2] Research center of building energy efficiency, Tsinghua university. Annual report on China building energy efficiency 2017;37-38 (in Chinese)

[3] U.S. Department of Energy, USA. Buildings Energy Data Book 2010.

[4] Agrawal, D. C. Efficiency and efficacy of incandescent lamps. American Journal of Physics 1996;64:649.

[5] Dubois MC, Blomsterberg Å. Energy saving potential and strategies for electric lighting in future North European, low energy office buildings: A literature review. Energy and Buildings 2011;43:2572-82.

[6] Dunne DA. Some effects of the quality of light on health. Journal of Orthomolecular Medicine 1989;229–323.

[7] U.S. Green Building Council. Green Building Rating Systems-Draft Recommendations for a U.S. Rating System 1995.

[8] Ullah I, Shin S. Highly concentrated optical fiber-based daylighting systems for multi-floor office buildings. Energy and Buildings 2014;72:246-261.

[9] Obianuju ON, Chong KK. High acceptance angle optical fiber based daylighting system using two-stage reflective non-imaging dish concentrator. Energy Procedia 2017;105:498-504.

[10] Ullah I, Whang JA. Development of optical fiber-based daylighting system and its comparison. Energies 2015;8:7185-7201.

[11] Tsangrassoulis A, Doulos L, Santamouris M. On the energy efficiency of a prototype hybrid daylighting system. Solar Energy 2005;79:56-64.

[12] Kandilli C, Ulgen K. Review and modelling the systems of transmission concentrated solar energy via optical fibers. Renewable and Sustainable Energy Reviews 2009;13:67-84.

[13] Lingfors D, Volotinen T. Illumination performance and energy saving of a solar fiber optic lighting system. Optics Express 2013;21:A642.

[14] Tekelioglu M, Wood BD. Thermal management of the polymethylmethacrylate (PMMA) core optical fiber for use in hybrid solar lighting. In: ASME 2003 International Solar Energy Conference American Society of Mechanical Engineers 2003;709-719.

[15] Kandilli C , Turkoglu AK , Ulgen K. Transmission performance of fibre-optic bundle for solar lighting. International Journal of Energy Research 2009;33:194-204.

[16] Ravi G, Meg T, Sean L. Design and development of a faceted secondary concentrator for a fiber-optic hybrid solar lighting system. Solar Energy 2017;157:629-

640.

[17] Tang S, Hong H, Jin H, Xuan YM. A cascading solar hybrid system for co-producing electricity and solar syngas with nanofluid spectrum selector. Applied Energy 2019;248:231-240.

[18] Qu W, Hong H, Jin H. A spectral splitting solar concentrator for cascading solar energy utilization by integrating photovoltaics and solar thermal fuel. Applied Energy 2019;248:162-73.

[19] Song J, Zhu Y, Tong K, Yang YP, Reyes-Belmonte MA. A note on the optic characteristics of daylighting system via PMMA fibers. Solar Energy 2016;136:32-34.

[20] Arnaoutakis GE, Marques-Hueso J, Mallick TK, Richards BS. Coupling of sunlight into optical fibres and spectral dependence for solar energy applications. Solar Energy 2013;93:235-43.

[21] Raj P, Subudhi S. A review of studies using nanofluids in flat-plate and direct absorption solar collectors. Renewable and Sustainable Energy Reviews 2018;84: 54-74.

[22] Brekke N, Dale J, Dejarnette D, Hari P, Orosz M, Roberts K, Tunkara E, Otanicar T. Detailed performance model of a hybrid photovoltaic/thermal system utilizing selective spectral nanofluid absorption. Renewable Energy 2018;123: 683-693.

[23] Hjerrild NE, Mesgari S, Crisostomo F, Scott JA, Amal R, Taylor RA. Hybrid PV/T enhancement using selectively absorbing Ag–SiO2/carbon nanofluids. Solar Energy Materials and Solar Cells 2016;147:281-287.

[24] Dejarnette D, Tunkara E, Brekke N, Otanicar T, Roberts K, Gao B, Saunders AE. Nanoparticle enhanced spectral filtration of insolation from trough concentrators. Solar Energy Materials and Solar Cells 2016;149:145-153.

[25] Sreekumar S, Joseph A, Kumar CS, Thomas S. Investigation on influence of antimony tin oxide/silver nanofluid on direct absorption parabolic solar collector. Journal of Cleaner Production 2020;249:119378.

[26] Chen N, Ma HY, Li Y, Cheng JH, Zhang CY, Wu DX, Zhu HT. Complementary optical absorption and enhanced solar thermal conversion of CuO-ATO nanofluids. Solar Energy Materials and Solar Cells 2017;162:83-92.

[27] Lan OY, Yu R. The development of wind-solar energy systems in China. International Conference on Energy & Environment Technology. IEEE Computer Society 2009.

[28] Wang C, Abdul-Rahman H, Rao SP. Daylighting can be fluorescent: Development of a fiber solar concentrator and test for its indoor illumination. Energy and Buildings 2010;42:717-727.

[29] Wen X, Wang S, Yang D. A preliminary study on the regional characteristics of solar radiation in China over the past 40 years. China meteorological society. Proceedings of the 2007 annual meeting of China meteorological society 2007:426-441.

(in Chinese)

[30] Gupta HK, Agrawal GD, Mathur J. Investigations for effect of Al2O3–H2O nanofluid flow rate on the efficiency of direct absorption solar collector. Case Studies in Thermal Engineering 2015;5:70-8.

[31] Chen ZX, Zheng D, Wang J, Chen L, Sundén B. Experimental investigation on heat transfer characteristics of various nanofluids in an indoor electric heater. Renewable Energy 2020;147:1011-1018.

[32] Zeng J, Xuan YM. Enhanced solar thermal conversion and thermal conduction of MWCNT-SiO2/Ag binary nanofluids. Applied Energy 2018;212:809-819.